Improving Off-angle Iris Recognition using Iris Quadrant Masking

Jitendra Sai Kota
School of Data Science and Analytics
Kennesaw State University
Marietta, USA 30060
Email: jkota@students.kennesaw.edu

Mahmut Karakaya
Department of Computer Science
Kennesaw State University
Marietta, GA 30060 USA
Email: mkarakay@kennesaw.edu

SoutheastCon 2022 | 978-1-6654-0652-9/22/$31.00 ©2022 IEEE | DOI: 10.1109/SoutheastCon48659.2022.9764073

Abstract*— Iris recognition using frontal eye images has been explored successfully by a lot of researchers. There are certain challenges to iris recognition such as corneal refraction, 3D iris texture, limbus occlusion, and blur, which are ignored in frontal iris recognition as their effects are minimal. However, those problems associated with iris recognition are amplified when designing biometrics based on off-angle iris images. As the gaze angle of the probe increases, the Hamming scores for intra-class comparisons are increased and the Hamming scores for inter-class comparisons are decreased, which causes an increased false-match rate. In this paper, our goal is to improve the recognition accuracy for off-angle images. We first investigated the Hamming distance scores in each quadrant of the iris pattern. Second, we masked each quadrant to determine if masking improves the accuracy. Based on our results, due to corneal reflection, masking the iris pixels in the quadrant at the 6 o'clock and 12 o'clock directions improve the performance of iris recognition in comparison to using the entire iris region for recognition.

***Keywords*— biometrics, iris recognition, off-angle, masking**

I. INTRODUCTION

Biometric identification of a person has become a reliable identification method in the last few years. Using a human's features for privacy rather than a password, which is susceptible to breaches, has turned out to be a safer option. Several biometric identification methods such as fingerprint scanning, voice recognition, facial recognition, and iris recognition have emerged in the past few years. Among all of them, iris recognition has turned out to be one of the better approaches due to the consistently low error rate. The irises of two different eyes are so separable that they can be used to distinguish two eyes of the same person or even two twins with the same DNA well. Also, iris recognition right now is inexhaustible as is evident from the fact that the world population is 7.9 billion, a number that would require less than 33 bits to represent everyone. On the other hand, iris scanners scan around 240 biometric features [1] showing us that the current iris recognition scanners can uniquely identify individuals even if the population were to grow 8 times to the present size. Also, iris recognition eliminates the necessity to conduct experiments on a diverse population set. The iris data is free from gender and ethnic differences as only the iris pattern are considered when identifying a person. Also, the color of the iris doesn't matter as the images are captured on an infrared camera. The additional advantage that iris recognition has when compared to biometric systems such as a fingerprint is that it is non-intrusive. With the world moving towards a more contact-free environment, iris recognition provides a better option than fingerprint scanners.

Most of the current iris recognition systems are derived from Daugman's iris recognition method [2]. This is a five-step process – iris capturing, iris segmentation, iris normalization, iris encoding, and iris matching. Iris is first captured using near-infrared cameras. Then, the iris region is segmented between the inner and outer iris boundaries. To counter for the distance between camera and eyes, pupil dilation, and zoom factor of the camera, the segmented iris is normalized into a rectangular shaped 2D block using polar coordinates. These normalized images are then encoded into binary iris codes using Gabor wavelet filters. Finally, the derived iris code is compared with the iris codes in the database using Hamming distances, and the matching is done. Iris images from the same person have Hamming distances close to 0, and the iris images of two different people have Hamming distances close to 0.5.

Although iris recognition is highly accurate for ideal frontal images, its accuracy drops dramatically for non-ideal images. Several factors such as reflections, occlusion, and including the gaze angle negatively affect the accuracy of the system. Current iris capturing systems reject images that are affected by those factors. This is the reason the current iris capturing systems require a controlled environment to capture the iris images. This limits the capability of iris recognition technology. Iris recognition can be extended to the use of identifying and tagging individuals on the go for security purposes in the future. If iris recognition must go beyond identification in a controlled environment, we should be able to overcome its challenges. Off-angle iris recognition is an emerging research area within the field of iris recognition that deals with capturing images taken at different gaze angles. Such biometric systems are referred to as Standoff iris biometric systems. These systems aim at identifying non-cooperative individuals in addition to cooperative individuals. Apart from reflections and gaze angle, off-angle iris images also suffer from other challenges such as corneal refraction, limbus occlusion, depth of field blur, and complex 3D structure of the iris.

This project was supported by NSF awards CNS-1909276 and 2100483.

A comparison of the intra-class and inter-class hamming distances between frontal and off-angle iris images of subjects revealed the impact the above challenges have on iris recognition. This information helped us explore a solution to better the performance of off-angle iris recognition. The remaining paper is organized as follows: Section II gives a brief overview of the related works. Section III describes the effect of eye structures in detail and outlines our methodology. Section IV has our experimental setup and the results. We finally conclude the paper in Section V.

II. RELATED WORKS

Several researchers have worked on iris recognition in the past. The most referred work in iris recognition is the Gabor phase-quadrant feature descriptor described by Daugman [2]. This technique uses spatial filters called Gabor filters which generate features from segmented iris images. These features represent the texture of the iris. These images are then normalized and then converted into a binary code comprising of only 1s and 0s, which is called the iris code. Hamming Distances are then calculated between these iris codes for different images and inter-class and intra-class distance measures are evaluated to identify an individual.

Traditionally, researchers focus on improving the performance of iris recognition by ignoring several challenging issues in off-angle iris images such as corneal refraction, depth of field blur, three-dimensional iris textures, and the limbus effect. When comparing iris images from the same angle, all the above issues have a similar effect. However, they affect the performance considerably in the case of off-angle iris images.

Daugman [3] proposed a preprocessing technique where affine transformation was used to correct a possible geometric deformation due to the gaze angle. However, the reconstruction process undermines the efficiency of this method. Zuo et.al.[4] proposed a method in which ellipses were fit to iris boundaries which helped correct the geometric deformation. Li et. al. [5] used SVM to classify iris images as frontal and off-angle based on the geometric features of corneal reflections. Then the features are learned independently for the two classifications. However, all these methods do not work beyond 30° as the effects due to eye structures are more intense at these angles.

Ray tracing method has been used by Price et. al. [6], Santos-Villalobos et. al. [7], which computes the refraction of light rays and estimates the region of impact on iris texture based on the angle. This method worked well for synthetic eye images but failed with real images due to other effects such as limbus occlusion. Karakaya et. al. investigated the effect of limbus occlusion [8] and three-dimensional iris structure [9] on off-angle iris images. Depending on the limbus height, the performance deteriorated for the same subject images in terms of increasing the Hamming Distances from 0.05 to 0.2. They have also noted that the hamming distances for the same subject increased from 0.02 to 0.1 as the gaze angle increased. They also stated that the corneal refraction effect alone increased the hamming distances from 0.05 to 0.25 for the same subject images. These studies emphasize the effect that limbus occlusion, the three-dimensional nature of iris, and corneal refraction have on images that are captured at higher off-angles.

In another study [10], they examined how the performance of iris recognition varied according to gaze angle based on the eye structures such as limbus, cornea, and aqueous humor. They have found that the intra-class hamming distances increased with an increase in the gaze angle of the probe image and the inter-class hamming distances decreased with the same trend in the gaze angle of the probe image. They also found that inter-class and intra-class hamming distance distributions got closer as the gaze angle increased.

III. METHODOLOGY

Some of the major challenges to biometric systems that use iris recognition are corneal refraction, limbus occlusion, the distortions caused due to the 3D structure of the iris, the depth of blur effect, and the occlusion due to eyelids. In frontal images, the probe image and the enrollment image are captured under similar conditions. So, all the above challenges cause similar distortions to the true iris structure. This explains the small Hamming distances obtained between objects of the same subject. The subject must stand in front of a camera until a proper iris image is captured in this case. However, standoff iris recognition systems are more flexible and do not require the subject to stand in front of the camera. As a result of such a setting, iris images are captured from different angles and these gaze angles amplify the effect of the limbus, corneal refraction, and three-dimensional iris texture.

Eye structures in the posterior eye affect the captured iris image [10]. Cornea and aqueous humor refract the light going through it concerning both the angle to the cornea and the image acquisition angle. The three-dimensional structure of the iris appears different in different angles. A tissue present between the cornea and sclera called limbus occludes the iris plane on the sides. The occlusion effect varies as the image acquisition changes. Synthetic eye images in Figure 1 show the effects of these eye structures on iris texture appearance in an off-angle image. The figure shows that corneal refraction of light affected the normalized iris image on the side that was the farthest from the camera. The three-dimensional iris texture contributed to the maximum distortion nearer to the pupil and the side nearest to the camera. Similarly, limbus occlusion affected the normalized image at 6 o'clock and 12 o'clock directions in the iris image. The images were blurred a lot in the central part of normalized images due to the depth of field, which is defined as the distance between the closest and the farthest sharp looking objects in a scene.

The above inferences inspired us to study these effects further on the recognition performance. Since the degradation of performance was mapped to certain portions of the normalized iris image, we first investigate their effects on the performance of iris recognition using Hamming distance analysis. Then, we propose to mask out the portions which severely affect the performance of iris recognition and use the remaining portions for iris recognition.

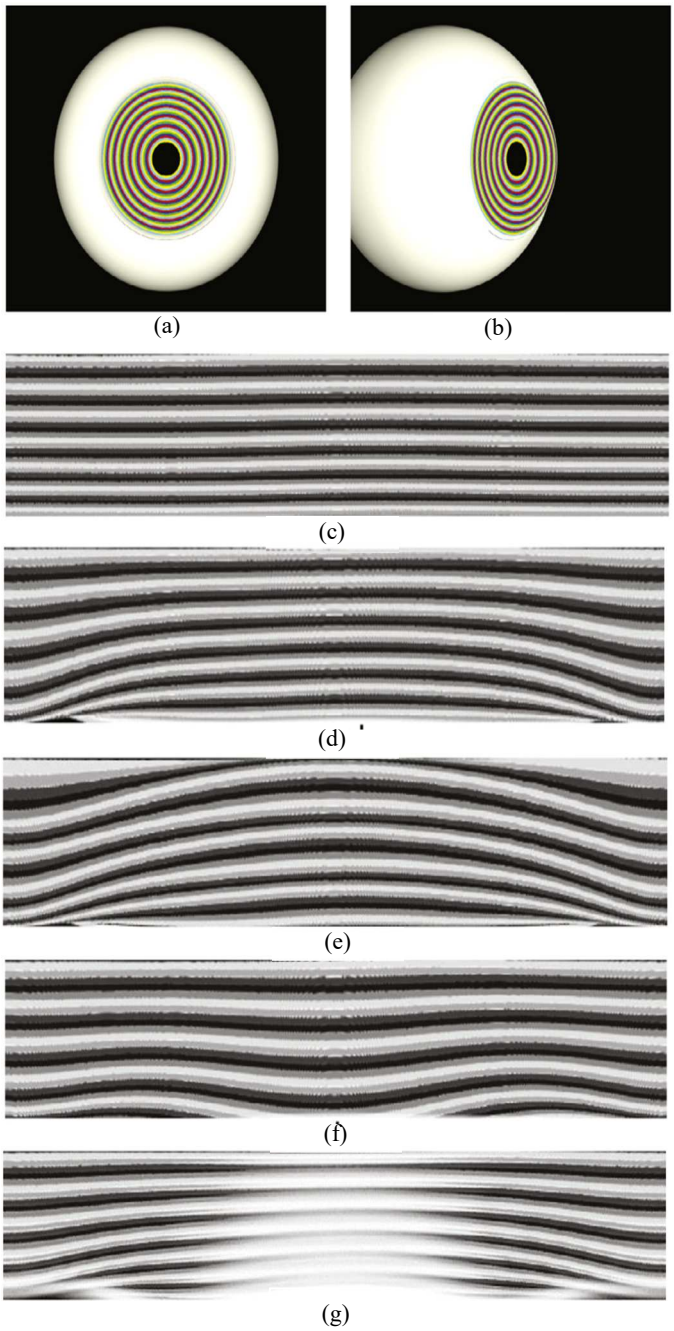

Figure 1: Synthetic eye images in (a) Frontal (b) off-angle (c) Normalized iris image in frontal image and Distortions in normalized iris due to (d) corneal refraction (e) 3D iris structure (f) limbus occlusion, and (g) depth of field blur.

To investigate the Hamming distance scores in different iris textures, we partition the iris pattern into four regions : 3 o'clock, 6 o'clock, 9 o'clock and 12 o'clock as shown in Figure 2(a). The corresponding normalized iris image is illustrated in Figure 2(b). The black horizontal line indicates the start of elliptical unwrapping in the normalized image. Since the iris normalization starts at the 3 o'clock direction, the normalized image is split at the 3 o'clock region into two parts. For

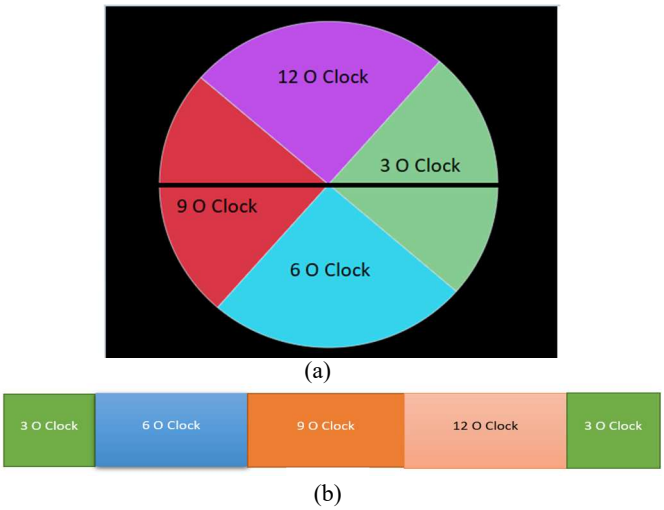

Figure 2: (a) Partitions in the circular iris structure (b) Partitions when translated to the normalized iris image.

computing the Hamming distance, we first keep one region and mask others by including masked regions in the mask of iris images. Hamming distance (HD) scores are calculated in traditional biometric systems as follows:

$$\mathrm{HD} = \frac{\|(c_A \otimes c_B) \cap (m_A \cap m_B)\|}{\|m_A \cap m_B\|} \quad (1)$$

where the logical XOR ($\otimes$) compares iris codes c, and logical AND ($\cap$) excludes occlusion masks m, from the calculation. The norm ($\|\ \|$) counts the number of bits.

To keep one region and mask others, we exclude other regions from Hamming distance (HD) calculation using masking approach as follows:

$$\mathrm{HDwR} = \frac{\|(c_A \otimes c_B) \cap (m_A \cap m_B) \cap (e_A \cap e_B \cap e_C)\|}{\|m_A \cap m_B \cap e_A \cap e_B \cap e_C\|} \quad (2)$$

where exclusion masks, e_A, e_B, and e_C can be eliminated from Hamming distance calculation as additional masks.

Investigating each region one by one highlights the region that severely affected the performance of iris recognition. Therefore, we can improve the recognition performance for off-angle iris images by eliminating these regions from the Hamming distance calculation and using the remaining portions.

IV. Dataset and Results

Frontal and off-angle iris images were captured from 100 individuals from -50 degrees to 50 degrees with an increment of 10 degrees [11]. The images were captured by near-infrared sensitive IDS-UI-3240ML-NIR cameras. Since 10 images are captured from each angle, there are 10,886 images from each eye. Off-angle images were captured by a moving camera. Ground truth segmentation was created for all images in the dataset using pupil, iris, and eyelid segmentation, where iris and pupil boundaries are segmented as ellipses and the eyelid boundary is fit using two quadratic curves. In this work, we

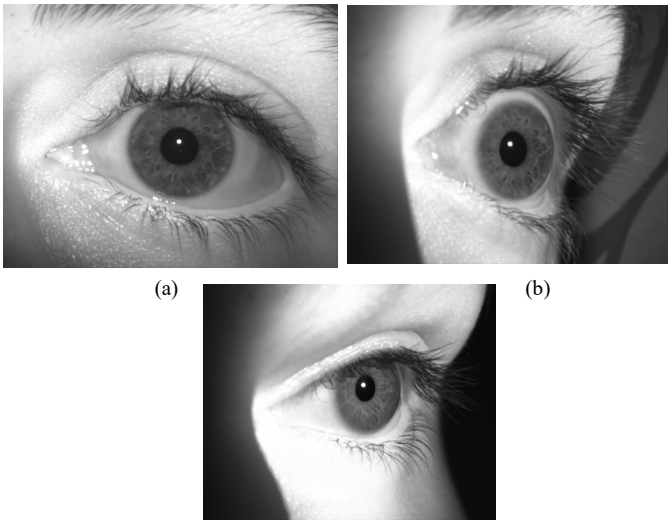

(a) (b) (c)

Figure 3: (a) Frontal iris image from s001, (b) Off-angle iris image at +40° in angle from s001 (c) Off-angle iris image at +40° angle from s002.

TABLE I: COMPARISON OF INTRA CLASS AND INTER CLASS HAMMING DISTANCES FOR TWO SUBJECTS

IRIS IMAGE COMPARISONS	HAMMING DISTANCES				
	ENTIRE IRIS	3 O'CLOCK	6 O'CLOCK	9 O'CLOCK	12 O'CLOCK
Intra-Class *s001 @ 0° vs. s001 @ 40°*	0.402	`0.389	0.467	0.363	0.385
Inter-Class *s001 @ 0° vs. s002 @ 40°*	0.501	0.478	0.488	0.548	0.368

include results for off-angle images from the left eye of each subject.

In our first set of experiments, we illustrate the effect of gaze angle deviation for off-angle iris images using three images. We first investigated how each region (i.e., 3 o'clock, 6 o'clock, 9 o'clock, and 12 o'clock) was performing individually on iris recognition using the pixels of only one region and comparing the Hamming distances between the frontal (0º in angle) and off-angle images (+40º in angle). For this purpose, we selected frontal and off-angle images from subject 1 (s001) and an off-angle image from subject2 (s002) as shown in Figure 3. We calculated Hamming distance scores for frontal and off-angle iris images using different regions. The hamming distance between the same subject is called intra-class (see Figure 3(a) and (b)) and the hamming distance between different classes is called inter-class (see Figure 3(a) and (c)) distance. The intra-class and inter-class Hamming distance scores are tabulated in Table I for the entire iris and each region separately. As shown in Table I, the entire iris texture shows intra-class distance as 0.402 and the inter-class distance as 0.501. Here the scores are close because of the comparison of images at frontal and off-angle. 3 o'clock and 9 o'clock regions perform better than entire iris scores as they have lower intra-class and higher inter-class Hamming distances. We observed that the 6 o'clock and 12 o'clock regions performed the worst as they cannot be distinguished apart using their intra-class and inter-class scores.

TABLE II: COMPARISON OF INTRA CLASS AND INTER CLASS HAMMING DISTANCES FOR 100 SUBJECTS

IRIS REGION CONSIDERATIONS	INTRA- CLASS HAMMING DISTANCES		INTER-CLASS HAMMING DISTANCES	
	MEAN	STANDARD DEVIATION	MEAN	STANDARD DEVIATION
Entire iris	0.309	0.101	0.489	0.018
3 o'clock	0.293	0.105	0.487	0.031
6 o'clock	0.330	0.126	0.488	0.029
9 o'clock	0.289	0.103	0.489	0.034
12 o'clock	0.346	0.117	0.494	0.061
3 and 9 o'clock	0.291	0.098	0.488	0.024

In our second set of experiments, we performed similar experiments for all the subjects in our dataset (100 subjects). Table II shows the mean and standard deviation scores of intra-class and inter-class for the entire iris, each separate region, and a combination of 3 and 9 o'clock. We observed a similar trend in the cumulative statistics derived from 100 subjects as in the first experiment. We observed that the average inter-class distances in each region have remained the same. However, the intra-class hamming distances were significantly higher for the 6 o'clock and 12 o'clock regions compared to the entire iris texture. In contrast, the 3 o'clock and 9 o'clock regions have smaller intra-class hamming distances than the entire region. This shows that 6 o'clock and 12 o'clock regions could be the bad regions that increase the overall mean score in the intra-class distribution. Therefore, we masked these two regions from the Hamming distance calculation in the 3 and 9 o'clock experiment. We observed an average intra-class score of 0.291 with a 0.098 standard deviation and an inter-class score of 0.488 with a 0.024 standard deviation. This approach helped us in decreasing the intra-class score and keeping the inter-class score the same when compared with the entire iris pattern.

Histograms of the Hamming distance distributions of intra-class and inter-class comparisons are shown in Figure 4 and Figure 5 for the entire iris, each separate region, and a combination of 3 and 9 o'clock. The histogram on the left with a green line represents comparisons between two images of the same subject (intra-class) and the red line represents comparisons between two different subjects (intra-class). Error can be visualized in the overlap between intra-class and inter-class Hamming distance plots. This overlap forms false reject and false match rates in the iris recognition where a threshold Hamming distance value is set to identify them. The distances coming from the same subject which lie to the right side of the distances coming from different subjects which lie to the left side of the threshold account for the false matches. We observed that the overlap of intra-class and inter-class distributions is much lower for 3 o'clock and 9 o' clock regions.

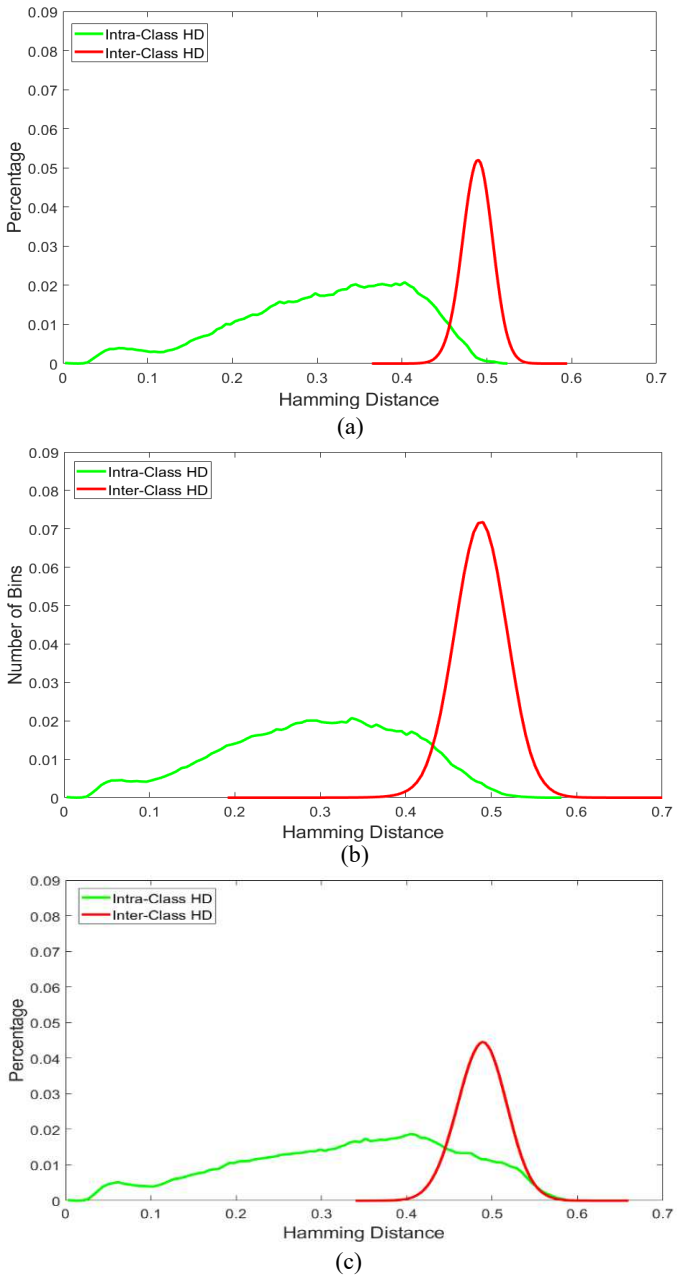

Figure 4: Histograms of Hamming distance comparisons for each iris images in our off-angle dataset. (a) entire iris region, (b) 3 o'clock quadrant, and (c) 6 o'clock quadrant. The histogram on the left with green line represents comparisons between intra-class and the red line represents comparisons between intra-class.

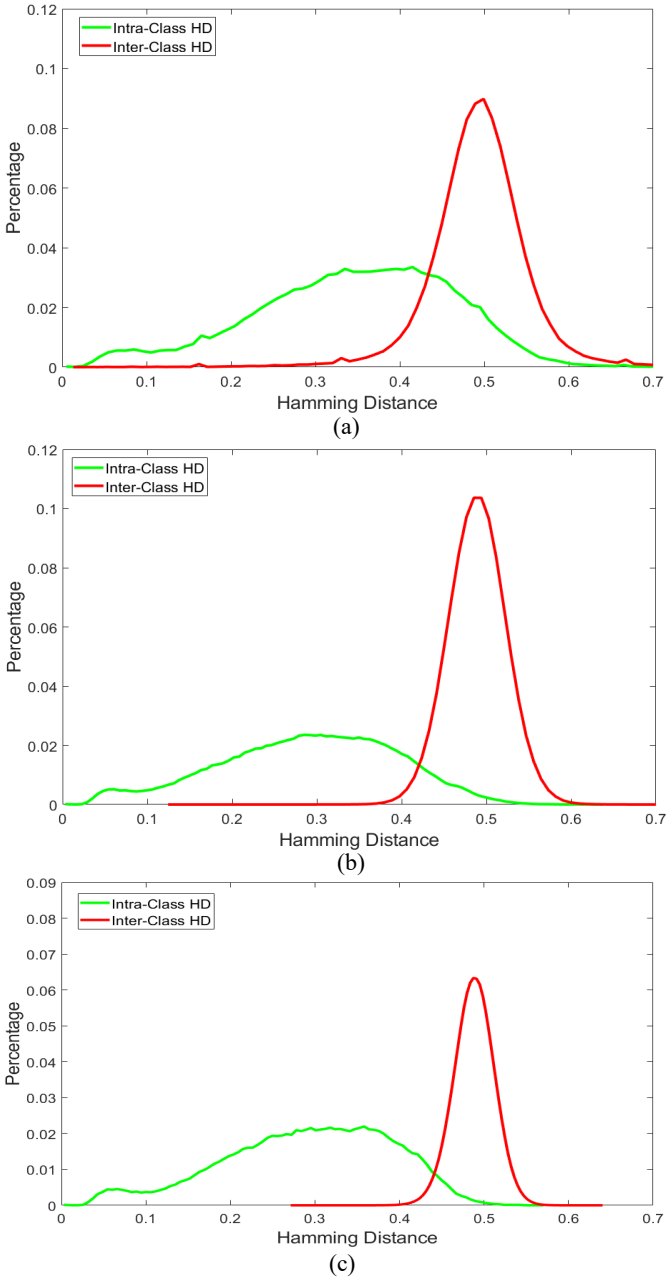

Figure 5: Histograms of Hamming distance comparisons for each iris images in our off-angle dataset. (a) 9 o'clock quadrant, (b) 12 o'clock quadrant, and (c) 3 o'clock & 9 o'clock quadrants. The histogram on the left with green line represents comparisons between intra-class and the red line represents comparisons between intra-class.

To compare the accuracy of different approaches, we also plot and calculate several metrics including receiver operating characteristic (ROC) curve and equal error rate (EER). ROC curves give a plot of true-positive rate (TPR) versus false-positive rate (FPR) at different thresholds with respect to final probability scores. EER is used to determine the error rate at a point where the false-positive and false-negative values become equal in a ROC curve. A curve closer to the upper left corner, having less error rate and low EER value is related to higher accuracies in experiments with comparisons.

Figure 6 compares the recognition performance at each quadrant region (3 o'clock, 6 o'clock, 9 o'clock, and 12 o'clock) in the iris. The ROC curves for 3 o'clock and 9 o'clock were closer to the top left corner. This showed their better performance compared to the 12 o'clock and 6 o'clock regions. As shown with a blue solid line, the 9 o'clock quadrant outperformed others with a 4.74% EER score. The second-best result was observed at the 3 o'clock region with a 5.51% EER (see blue dotted line). The 12 o'clock and 6 o'clock regions showed lower accuracy with a high EER at 19% and 23%,

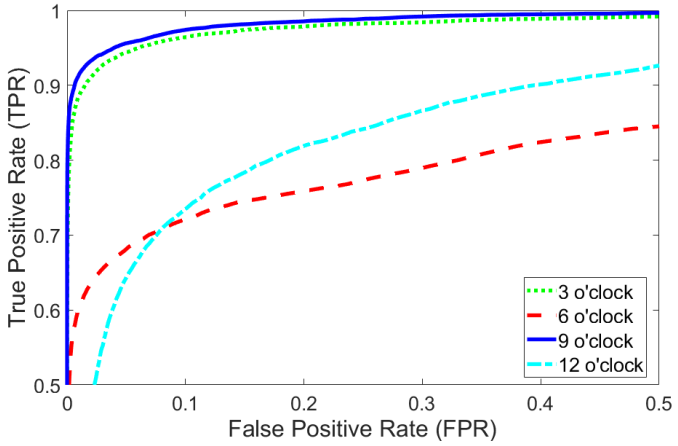

Figure 6: Comparison of recognition performances using ROC curves for 3 o'clock, 6 o'clock, 9 o'clock, and 12 o'clock regions.

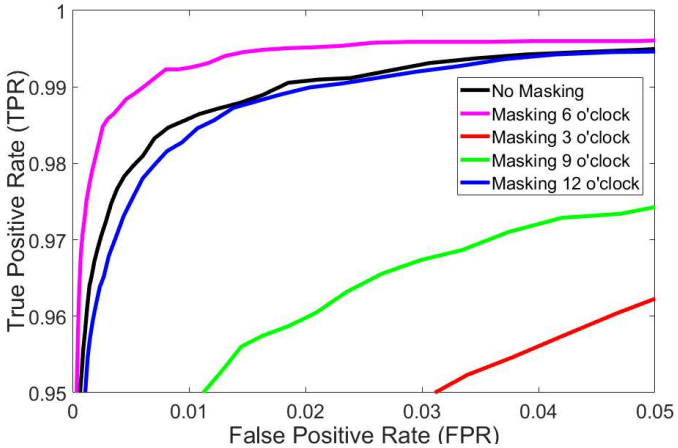

Figure 7: Performance analysis using ROC curves for iris recognition comparing the performance of masking one of the quadrant regions.

respectively. From these results, we concluded that the 6 o'clock region was the worst-performing among all regions.

The main reason for the 6 o'clock region being worse than the 12 o'clock region is the eyelid segmentation masking the portion of the iris covered by the eyelids. This phenomenon is not so common with the iris at 6 o'clock region which remains exposed to the camera even in off-angles. There is not much to differentiate between the regions 3 o'clock and 9 o'clock. However, the 9 o'clock region appears to be faring slightly better than the 3 o'clock region. The corneal refraction effect is more in the 3 o'clock region than in the 9 o'clock region. Limbus occlusion occurs more in the 9 o'clock region than in the 3 o'clock region. This shows that corneal refraction creates stronger distortions than limbus occlusion for off-angle images. The second set of experiments revealed the extent of iris distortions in each quadrant region for the off-angle images.

Using these results, we designed our third set of experiments where we masked one of the four regions at a time and kept the remaining three regions to check if that would improve the performance when compared with the baseline result (i.e., no masking or entire iris). Figure 7 shows the performance analysis using ROC curves for the iris recognition comparing the performance of masking one of the quadrant regions and baseline result without masking. We observed that the performance of iris masking of the 6 o'clock region was better than the baseline result where their EER scores are 0.8021% and 1.249%, respectively. This suggests that masking the 6 o'clock region could be a good way to improve the recognition performance of off-angle iris images. Masking the 12 o'clock quadrant produced a close result to the baseline with an EER of 1.251%. We also observed that masking either 3 o'clock or 9 o'clock regions degraded the recognition performance considerably where their EER scores are 4.215% and 3.167%, respectively. This indicates that iris texture in the 3 o'clock and 9 o'clock regions is less affected by the gaze angle compared with the 6 o'clock and 12 o'clock regions.

V. Conclusion

This paper investigated the performance of iris recognition for off-angle iris images through masking of sub regions in the iris. The entire iris region was split into 4 sub-regions: 3 o' clock, 6 o'clock, 9 o'clock, and 12 o'clock based on their alignment. The sub-regions 9 o'clock and 3 o' clock turned out to contain the least affected iris pixels with lower EER scores. The 12 o'clock and 6 o'clock regions were affected the most with higher EER scores. This showed that iris recognition in off-angle images performs better by masking the 6 o'clock and 12 o'clock regions. The masking of 6 o'clock region provided better EER scores than the baseline result using the entire iris region. We observed that corneal refraction creates stronger distortions than limbus occlusion for off-angle images. Therefore, masking the iris pixels in the quadrant at the 6 o'clock and 12 o'clock directions improve the performance of iris recognition instead of using the entire iris.

References

[1] S. Simhadri, S. James, and B. Fuller. "Cryptographic Authentication from the Iris", Information Security , pp. 465-485, September 2019,.

[2] J.Daugman, "How iris recognition works" , IEEE Trans. Circuits and Syst. Video Technol., vol. 14, no. 1, pp. 21–30, January 2004.

[3] J. Daugman, "New Methods in iris recognition," IEEE Transactions on Systems, Man, and Cybernetics, Part B (Cybernetics), vol. 37, no. 5, pp. 1167-1175, October 2007.

[4] J. Zuo, N. D. Kalka, and N. A. Schmid, "A Robust IRIS Segmentation Procedure for Unconstrained Subject Presentation", Biometrics Symposium: Special Session on Research at the Biometric Consortium Conference, pp. 1-6., 2006.

[5] X.Li, L.Wang, Z.Sun, and T.Tan, "A feature-level solution to off-angle iris recognition", Proceedigs of International Conference on Biometrics, pp.1–6, 2013.

[6] J.R. Price, T.F. Gee, V. Paquit, K.W. Tobin, "On the efficacy of correcting for refractive effects in iris recognition", IEEE Conference on Computer Vision and Pattern recognition, , pp. 1-6, July 2007.

[7] H. J. Santos-Villalobos, D. R. Barstow, M. Karakaya, C. B. Boehnen and E. Chaum, "ORNL biometric eye model for iris recognition," IEEE Fifth International Conference on Biometrics: Theory, Applications and Systems (BTAS), , pp. 176-182, 2012.

[8] M. Karakaya, D. Barstow, H. Santos-Villalobos, and J. Thompson, “Limbus impact on off-angle iris degradation” , pp. 1-6, International Conference on Biometrics, 2013.

[9] G.N. Cerme, M. Karakaya, “Effects of 3D Iris Texture on Off-angle Iris Recognition”, Proceedings of IEEE 23rd Conference of Signal Processing and Communication Applications (SIU 2015), May 2015.

[10] M. Karakaya, “A Study of how gaze angle affects the performance of iris recognition”, Pattern recognition Letters,vol. 82, pp 132–143, 2016.

[11] M. Karakaya, D. Barstow, H. Santos-Villalobos and J. Thompson, "Limbus impact on off-angle iris degradation," International Conference on Biometrics (ICB), 2013, pp. 1-6.